Supplemental information for

α-Synuclein penetrates mucin hydrogels despite its mucoadhesive properties

Matthias Marczynski[a,#], Carolin A. Rickert[a,#], Slav A. Semerdzhiev[b], Wouter R. van Dijk[b], Ine M.J. Segers-Nolten[b], Mireille M.A.E. Claessens[b], and Oliver Lieleg[a,*]

[a] Department of Mechanical Engineering and Munich School of Bioengineering,
Technical University of Munich, Boltzmannstrasse 11, 85748, Garching, Germany

[b] Nanobiophysics, Faculty of Science and Technology,
University of Twente, Enschede, the Netherlands

*: correspondence: oliver.lieleg@tum.de

#: equal contribution

1. Refined estimation of the polypeptide net charge of all αSN variants used in this study

In the main manuscript, the net charge of αSN and the synthetic peptides was estimated by assuming full elementary charges per amino acid (if the pKa value of the respective amino acid was above/below pH 4). For a more detailed estimation, we here used two different protein calculators (public domain software): **Protein Calculator v3.4** (http://protcalc.sourceforge.net/, 10/24/2019) and **Prot pi** (https://www.protpi.ch/Calculator/ProteinTool, 10/24/2019). For both estimations, the amino acid sequence of wildtype α-synuclein was used[1]:

MDVFMKGLSK AKEGVVAAAE KTKQGVAEAA GKTKEGVLYV GSKTKEGVVH GVATVAEKTK EQVTNVGGAV VTGVTAVAQK TVEGAGSIAA ATGFVKKDQL GKNEEGAPQE GILEDMPVDP DNEAYEMPSE EGYQDYEPEA.

Depending on the algorithm used, different net charge values for the αSN protein were obtained. Those values are summarized in the following table:

Table S1: Estimated net charge of the five αSN variants used in this study. Values were determined for a pH level of 4.0 using the protein calculators listed in the tables. The calculated net charges are in good agreement with the determined net charge when elementary charges are assigned to amino acid side chains that are positively (Arg, His, Lys) and negatively charged (Asp) at pH 4.0.

	net charge		
α-synuclein variant	assuming full elementary charges	according to *Protein Calculator v3.4*	according to *Prot pi*
wild type αSN	+ 10	+ 9.3	+ 8.9
αSN 1-60	+ 12	+ 10.1	+ 10.2
αSN 1-108	+ 16	+ 12.7	+ 12.7
αSN 60-140	- 2	- 0.7	- 1.2
αSN A30P	+ 10	+ 9.3	+ 8.9

With all three approaches, comparable results are obtained. However, we would like to emphasize that none of those calculator software applications take any possible tertiary or quaternary protein conformations into account (which might be negligible for unstructured proteins such as αSN), nor do they consider inductive effects (which might be very well relevant for a αSN polypeptide).

---

[1] UniProtKB – accession number P37840 (10/24/2019)

2. Comparison of fluorescence peak positions and positions of visual changes in phase contrast images of Fig. 1

The data shown in Fig.1a and b stem from two different measurements, in which the image acquisition times were different. For the first measurement, only fluorescence images were acquired to analyze the intensity profiles during the penetration of αSN into the mucin hydrogel. During those experiments, changes within the hydrogel structure were observed in phase contrast microscopy but not sufficiently documented for all time steps. That is why another set of experiments was conducted with the goal to colocalize the intensity maxima and the internal interface observed in phase contrast images. As shown in the figure below, the fluorescence intensity maxima show the same time dependency for both measurements.
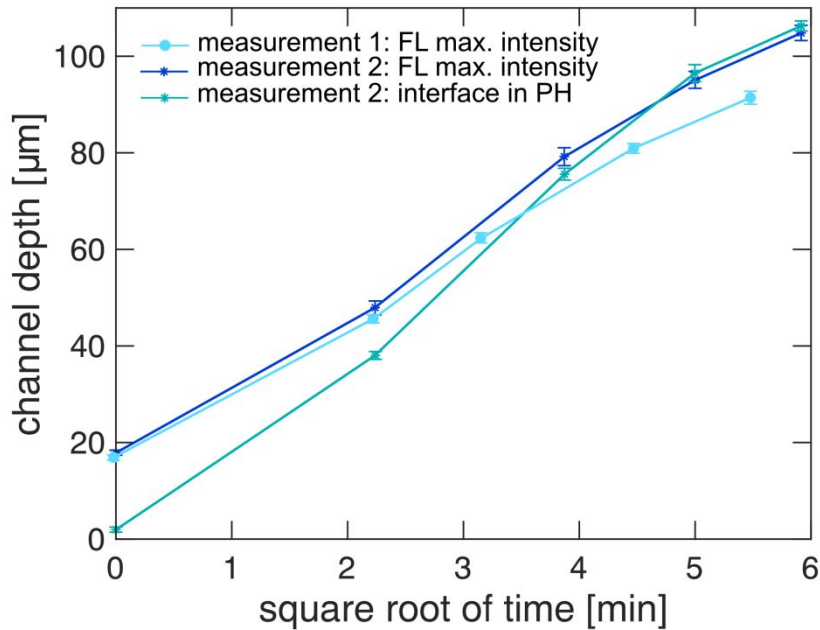

Figure S1: Positions of fluorescence intensity maxima and the internal gel interface visible in phase contrast images. The position of the fluorescence intensity maxima of the first measurement (bright blue line) and the second measurement (dark blue line) are plotted against the square root of time. The data from both measurements shows a time dependency of the peak position matching a root function. The positions of the internal gel interface that is visible in phase contrast images of measurement 2 is displayed in turquois.

3. MST measurements of wildtype αSN and two mutant variants at different temperatures
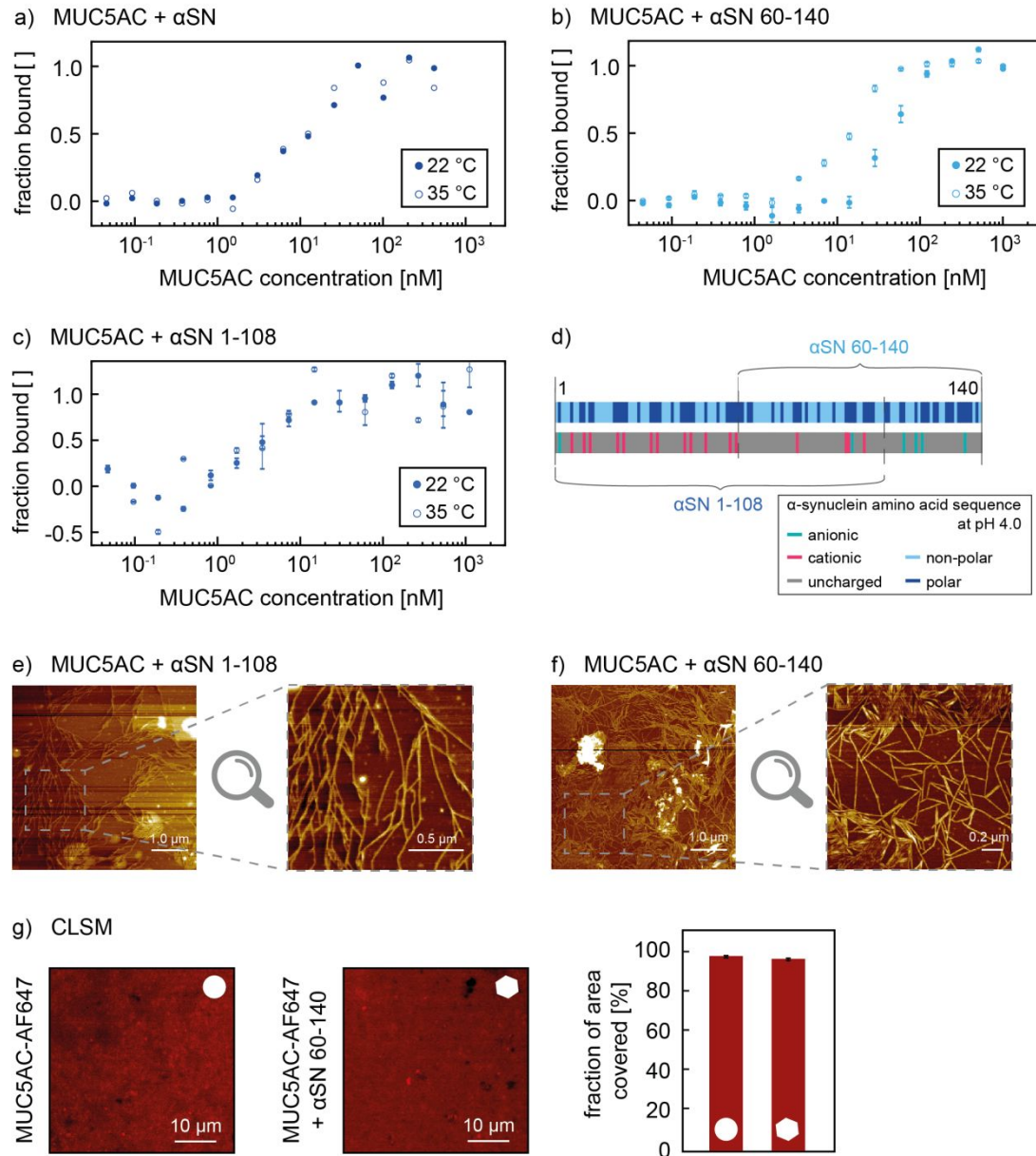

Figure S2: Mucin binding to different αSN variants as determined by MST and AFM. The binding affinity of wildtype αSN and C-terminal truncated αSN 1-108 is independent of the ambient temperature (**a, c**). In contrast, the binding affinity of the N-terminal truncated αSN 60-140 exhibits a temperature dependency (**b**). The structure of the two αSN is visualized in the charge and polarity maps shown for pH 4.0 (**d**). AFM images of MUC5AC molecules incubated that have been incubated with αSN 1-108 (**e**) and αSN 60-140 (**f**), respectively, further demonstrate that both αSN variants can bind to mucin molecules. αSN 60-140 does not induce bundling of

MUC5AC fibrils (**g**). The area fraction covered with fluorescent structures was determined and averaged for four frames (*n* = 4). Error bars denote the standard deviation.

MST measurements are conducted both at room temperature (i.e., 25 °C) and at physiological body temperature (i.e., 37 °C). An altered binding affinity at an elevated temperature is only observed for αSN 60-140. This αSN mutant variant lacks the cationic N-terminal domain and thus exhibits a negative net charge even at pH 4.0; however, it comprises a large number of hydrophobic amino acids. The binding affinity of wildtype αSN and αSN 1-108 is not affected by an increase in temperature. Since only hydrophobic interactions but not electrostatic interactions exhibit a temperature dependency, this indicates that the mucoadhesive properties of αSN 60-140 might not be dominated by electrostatic interactions. In contrast, for the other two αSN variants – which both carry a large number of cationic binding sites – binding interactions seem to be dominated by electrostatic forces.

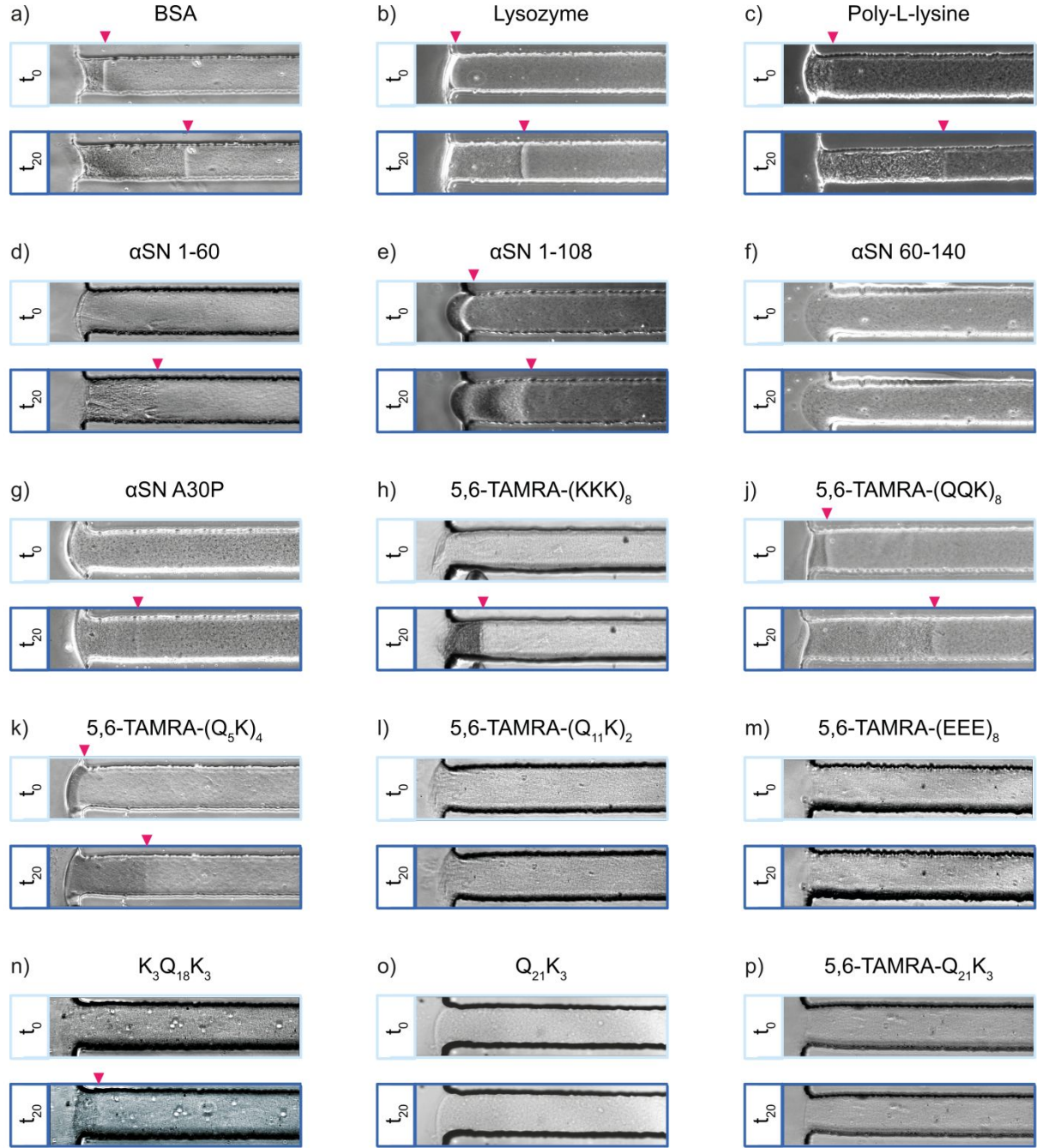## 4. Phase contrast images of MUC5AC gels after penetration of different proteins and peptides

Figure S3: Phase contrast images of MUC5AC gels after injection of proteins/peptides (t_0) and twenty minutes thereafter (t_{20}). The penetration of natural proteins (**a-c**), αSN mutants (**d-g**), and synthetic peptides (**h-p**) was investigated. For each condition, at least three chips ($n \geq 3$) were evaluated.

Phase contrast images of the MUC5AC hydrogels were acquired after injection of the test molecules into the test reservoir. We refer to the time point of the acquisition of the first image as t_0. However, due to necessary adjustments of imaging settings after sample injection, the time between sample injection and acquisition of the first image differs between the different experiments, and we therefore sometimes detected an internal gel/gel interface even for images already at t_0.

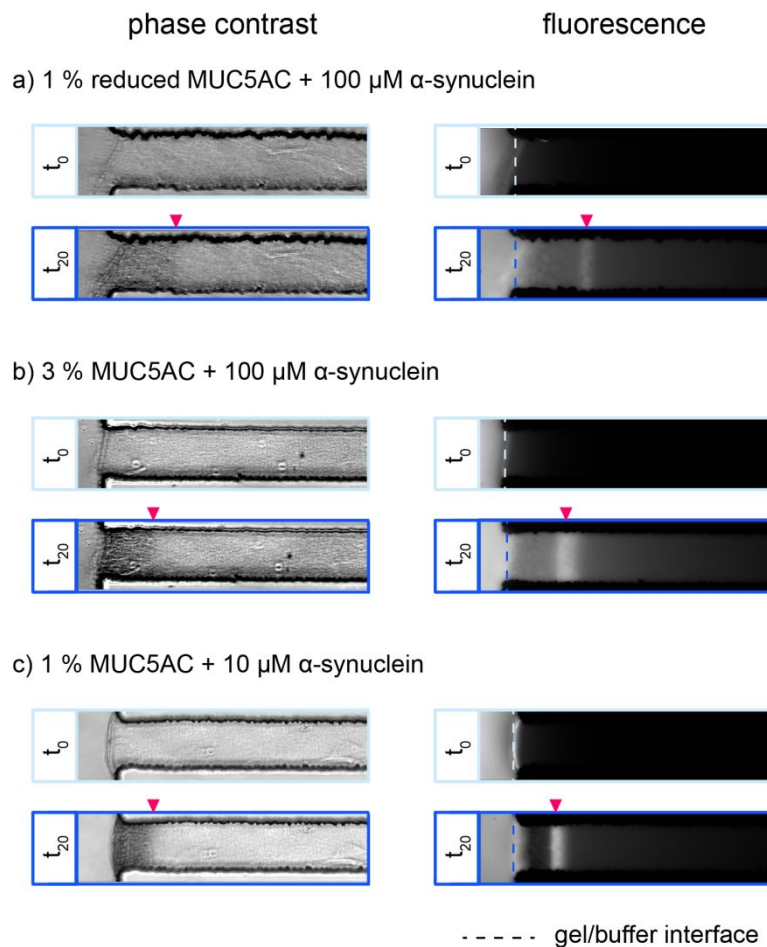## 5. αSN-induced rearrangement of MUC5AC gels at different conditions

Figure S4: αSN-induced rearrangement of the MUC5AC gel microarchitecture at different conditions. **a)** For a 10 times lower concentration of αSN (10 µM) than in the previous experiments (100 µM) the rearrangement of the mucin gel structure can still be observed in phase contrast images. **b)** Even at a physiological mucin concentration of 3 % (w/v), αSN rearranges the hydrogel network. **c)** Mucin hydrogels reconstituted in the presence of 1 mM of the reducing agent DTT are also restructured by αSN. Arrows indicate the position of the internal gel/gel interfaces and dotted lines indicate the position of the gel/buffer interface in fluorescence images. For each condition, at least two chips ($n \geq 3$) were evaluated.